

Received June 4, 2018, accepted July 8, 2018, date of publication July 12, 2018, date of current version August 7, 2018.

Digital Object Identifier 10.1109/ACCESS.2018.2855420

# Combining Convolutional Neural Network and Distance Distribution Matrix for Identification of Congestive Heart Failure

YAOWEI LI<sup>1\*</sup>, YAO ZHANG<sup>2,3\*</sup>, LINA ZHAO<sup>4\*</sup>, YANG ZHANG<sup>5\*</sup>, CHENGYU LIU<sup>1</sup> , LI ZHANG<sup>6</sup>, (Member, IEEE), LIUXIN ZHANG<sup>5</sup>, ZHENSHENG LI<sup>5</sup>, BINHUA WANG<sup>7</sup>, EYK NG<sup>8</sup>, JIANQING LI<sup>1</sup>, AND ZHIQIANG HE<sup>5</sup>

<sup>1</sup>State Key Laboratory of Bioelectronics, Jiangsu Key Laboratory of Remote Measurement and Control, School of Instrument Science and Engineering, Southeast University, Nanjing 210096, China

<sup>2</sup>Institute of Computing Technology, Chinese Academy of Sciences, Beijing 101408, China

<sup>3</sup>University of Chinese Academy of Sciences, Beijing 101408, China

<sup>4</sup>School of Control Science and Engineering, Shandong University, Jinan 250000, China

<sup>5</sup>Lenovo Research, Beijing 100085, China

<sup>6</sup>Computational Intelligence Group, Northumbria University, Newcastle upon Tyne NE1 8ST, U.K.

<sup>7</sup>Medical Big Data Center, Chinese PLA General Hospital, Beijing 100039, China

<sup>8</sup>School of Mechanical and Aerospace Engineering, College of Engineering, Nanyang Technological University, Singapore 639798

Corresponding authors: Chengyu Liu (chengyu@seu.edu.cn) and Zhiqiang He (hezq@lenovo.com)

\*These four authors contributed equally to this work.

This work was supported in part by the National Natural Science Foundation of China under Grant 61571113 and Grant 61671275, in part by the Key Research and Development Programs of Jiangsu Province under Grant BE2017735, in part by the Fundamental Research Funds for the Central Universities under Grant 2242018k1G010, and in part by the Southeast-Lenovo Wearable Heart-Sleep-Emotion Intelligent Monitoring Lab.

**ABSTRACT** Congestive heart failure (CHF) is a serious pathophysiological condition with high morbidity and mortality, which is hard to predict and diagnose in early age. Artificial intelligence and deep learning combining with cardiac rhythms and physiological time series provide a potential to help in solving it. In this paper, we proposed a novel method that combines a convolutional neural network (CNN) and a distance distribution matrix (DDM) in entropy calculation to classify CHF patients from normal subjects, and demonstrated the effectiveness of this combination. Specifically, three entropy methods were used to generate the distribution matrixes from a 300-point RR interval (i.e., the time interval between the successive cardiac cycles) time series, which are Sample entropy, fuzzy local measure entropy, and fuzzy global measure entropy. Then, three high representative CNN models, i.e., AlexNet, DenseNet, and SE\_Inception\_v4 were chosen to learn the pattern of the data distributions hidden in the generated distribution matrixes. All data used in our experiments were gathered from the MIT-BIH RR Interval Databases (<http://www.physionet.org>). A total of 29 CHF patients and 54 normal sinus rhythm subjects were included in this paper. The results showed that the combination of FuzzyGMEn-generated DDM and Inception\_v4 model yielded the highest accuracy of 81.85% out of all proposed combinations.

**INDEX TERMS** Congestive heart failure (CHF), convolutional neural network (CNN), distance distribution matrix (DDM), heart rate variability (HRV), entropy.

## I. INTRODUCTION

Congestive heart failure (CHF) is a serious pathophysiological condition, which has become a common cause of hospitalization with significant morbidity and mortality [1]–[4]. However, heart failure remains insufficiently diagnosed worldwide, especially in early age [5]–[8]. Precise diagnosis is thus vital for heart failure treatment. Previous studies showed that heart rate variability (HRV), which is associated

with the mortality of CHF, is an effective feature for discriminating CHF patients from normal subjects [9]–[11]. Over the past years, various machine learning methods were proposed to diagnose patients suffering from CHF based on HRV. For example, Isler and Kuntalp [12] proposed a model based on k-nearest neighbor classifier (KNN) and wavelet entropy. Jovic and Bogunovic [13] utilized random forest and combinations of linear and nonlinear features of HRV.

La Rovere *et al.* [11] designed a classifier based on regression tree with selected RMSSD, total power, HF, and LF/HF as useful classification features. There are also researchers who employed SVM and combinations of several HRV features and achieved relatively high accuracies [14]–[16].

Most existing works employ classifiers with comparatively simple structures and trained on small data sets. The input of their classifiers is empirically a set of selected features. However, the performance of the classifiers is largely based on feature selection processes [12], [14]. Thus in most cases, a large amount of time and effort is paid to manually find better feature subsets and even adopted the so-called exhaustive search methods to find the best subsets of features [17]. Additionally, the choice of the best feature combination may change with different datasets. With the explosion of data and the development of smart wearable devices, deep learning is a desirable way to overcome the shortage of artificial feature extraction and selection. Deep neural networks are designed to automatically learn the underlying hidden feature combinations without any manual process. As one type of the most successful deep neural network, convolutional neural network (CNN) has gained significant development and achieves state-of-the-art results on various tasks [11]. CNNs are able to accept raw and complete images as inputs, so as to avoid the risk of losing valuable information. Thus, we decide to employ different CNNs to automatically learn effective features from HRV data and produce accurate classification results without complicating manual feature extraction.

Entropy is a non-linear HRV analysis method, which provided a better understanding for the underlying mechanisms of the cardiovascular system [18]–[20]. In previous study, entropy calculation was able to distinguish CHF and normal sinus rhythm (NSR) subjects with appropriate parameters. A statistical significance for the two groups was obtained [21], [22]. Jovic and Bogunovic [13] tried to use combinations of entropy calculation results as the input of classifiers and acquired a moderate result of approximate 73% accuracy. It could be attributed to the simple and rough entropy calculation, i.e. there will be only a number value result, leading to a potential risk to lose useful information for subsequent normal/abnormal classification.

The construction of distance distribution matrix (DDM) is an essential step for entropy calculation. The difference between normal and abnormal cardiac conditions can be depicted and observed by DDM. This is thus a desirable input for CNN as it reveals the features of HRV signals in the manner of entropy analysis but contains richer information than a simple single entropy value calculation. The RR interval is the time interval between the successive cardiac cycles and regarded as an important feature of an ECG signal. It is usually quantified by the time difference between the occurrence of the maximum wave, i.e. the R wave of a cardiogram. Thus RR interval time series in the long-term RR Interval Databases from <http://www.physionet.org> [23] are used in this study to generate the DDMs.

In this study, our main aim is to use the DDM as an image feature to achieve classification between the NSR and CHF subjects by employing these improved representative CNN methods. Several stages were included in this study. The first stage is to convert RR interval time series into DDMs using three kinds of entropy methods: i.e. Sample entropy (SampEn), fuzzy local measure entropy (FuzzyLMEn) and fuzzy global measure entropy (FuzzyGMEn). The second stage is to train classifiers based on three different types of CNN models. Experimental study is presented in the last stage, which evaluates our models on two schemes. Our contributions are summarized as follows:

- 1) We improve three different types of classifiers without manual feature extraction based on latest state-of-art CNN models.
- 2) We generate three kinds of DDMs from RR interval time series as the input of these classifiers and compare their classification results based on the three CNN classifiers. All three kinds of DDMs show discriminability for the RR interval time series between NSR and CHF groups, and the performance of each model has no significant difference. This verifies the effectiveness of combination of DDM and the CNN model.
- 3) We choose the subject-based and segment-based schemes as the evaluation schemes and compared their performances. In this study, the segment-based scheme performs similarly to the subject-based scheme.

## II. CNN MODELS

AlexNet [24], DenseNet [25] and Inception\_v4 [26] were used in this study. AlexNet is one of the largest CNNs trained on the subsets of ImageNet used in the ILSVRC-2010 and ILSVRC-2012 competitions. DenseNet alleviates the disappearance of gradients and enhances feature propagation by encouraging feature reuse, and this greatly reduces the amounts of parameters. Inception\_v4 was one of several follow-up versions to GoogLeNet [27], and is the winner of ILSVRC 2014, but became deeper and wider by introducing residual connections and has a more simplified architecture and more inception modules than the previous versions [26]. All these models are representative CNN models. The details of the three employed CNNs as described as follows:

### A. ALEXNET

Original AlexNet contains five convolutional and three fully-connected ones. In our study, we converted those fully-connected layers into convolutional layers. This made it possible to efficiently run the CNN on  $297 \times 297$  input images. The architecture was summarized in Fig. 1. Firstly, we use a convolution with 64 output channels and kernel size  $11 \times 11$  to input distribution matrix followed by a  $3 \times 3$  max pooling layer. After several convolution and max pooling operations, dropout layers were also used to enhance the robustness of the model. At the end of the network, the global average pooling layer is performed. Besides, rectified linear units (ReLUs)

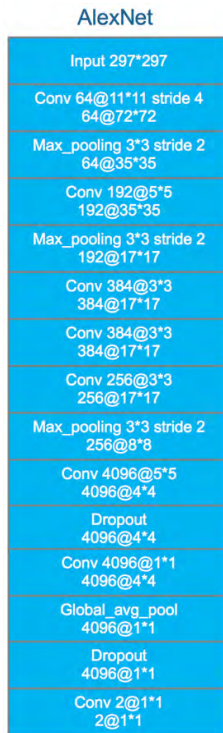


FIGURE 1. The architecture of AlexNet.

were used to reduce training time and local normalization scheme was used to aid generalization.

**B. DENSENET**

DenseNet consists of alternating transition layers and dense blocks. Fig. 2 illustrates the architecture of the DenseNet. Firstly, we use a convolution with 48 output channels followed by a transition layer. Each transition layer is to change the size of feature maps by convolution and pooling between dense blocks, which consists of a batch normalization layer, a ReLU layer and a  $1 \times 1$  convolutional layer with 24 output channels followed by a  $2 \times 2$  average pooling layer. In a dense block, each layer obtained additional inputs from all its preceding layers and passes on its own feature maps to all its subsequent layers. The network is divided into multiple densely connected dense blocks. At the end of the DenseNet, a global average pooling is used and then a softmax classifier is performed.

**C. INCEPTION-V4**

The main contribution of Inception\_v4 was the Inception Module that dramatically reduced the number of parameters in the network. Additionally, it used average pooling instead of fully connected layers at the top of the ConvNet, eliminating a large number of parameters without remarkably decrease of performance. In our study, we add ‘‘Squeeze-and-Excitation’’ (SE) block in each inception block to model channel-wise relationships in a computationally efficient manner. It enhance the representational power of modules



FIGURE 2. The architecture of DenseNet.

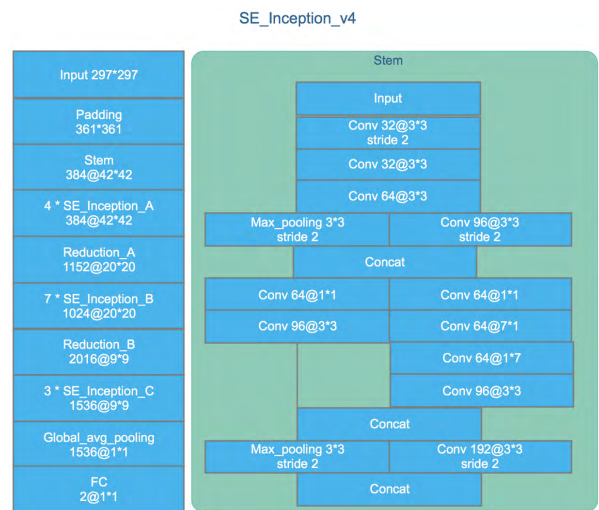


FIGURE 3. The whole architecture of SE\_Inception\_v4 and the ‘‘stem’’ module in SE\_Inception\_v4.

throughout the network. Consequently, we term our model as SE\_Inception\_v4. The overview of SE\_Inception\_v4 is illustrated in the left side of Fig. 3. It is composed of ‘‘stem’’, ‘‘inception’’ and ‘‘reduction’’ modules, as shown in Fig. 3 and Fig. 4 in detail.

**III. EXPERIMENT**

**A. DATA**

All data used in our experiments were gathered from the long-term RR Interval Databases (<http://www.physionet.org>) [23],



**FIGURE 4.** “Inception” and “Squeeze-and-Excitation” modules in SE\_Inception\_v4.

a free-access, on-line archive of physiological signals. The NSR RR Interval Database was used as the non-pathological and control group data. This database included 54 long-term RR interval recordings of subjects in normal sinus rhythm aged from 29 to 76. The CHF RR Interval Database was used as the pathological group data. This database included 29 long-term RR interval recordings of subjects aged from 34 to 79, with congestive heart failure (NYHA classes I, II, and III). The original ECG signals for both NSR and CHF RR interval databases were resampled at 128 Hz, and the beat annotations were obtained by automated analysis with manual review and correction.

**B. PRE-PROCESS**

RR interval is one of the important features of the ECG signal. It is the time interval between the successive cardiac cycles, which is usually quantified by the time difference between the occurrence of the maximum wave, R, of a cardiogram and is often called RR interval. In this section, two steps were used in the pre-process procedure for each RR interval recording:

*Step 1:* Each beat in the raw ECG signals was annotated as a normal or abnormal heartbeat. These abnormal heartbeats, usually caused by the ectopic beats such as supra-ventricular ectopic beats or ventricular ectopic beats (depending on the localization of the ectopic focus), were removed from the raw ECG signals, as the RR intervals formed from the abnormal heartbeats could confound the entropy analysis of HRV. We also remove RR intervals greater than 2 seconds to ignore the influence from the artifacts. Table 1 shows the total number of RR intervals for both NSR and CHF groups, as well as the numbers of RR intervals after the above procedure.

*Step 2:* Then we divide these ECG signals into several RR segments. The length of each RR segment is recorded as N, and we set N = 300, i.e. each RR segment contains 300 RR intervals.

**TABLE 1.** Statistical results of the numbers of RR interval recordings, RR intervals and RR segments from the 54 NSR and 29 CHF RR Interval Databases.

Variables	NSR group	CHF group
Name of RR interval recordings	NSR001-NSR054	CHF201-CHF229
No. of RR interval recordings	54	29
No. of RR intervals	5,790,504	3,312,195
No. of RR intervals after removing greater than 2s	5,780,148	3,306,394
No. of RR intervals after removing abnormal heartbeats	5,738,937	3,102,120
No. of RR segments when setting N=300	19,101	10,324

**C. GENERATION OF DDM**

SampEn [28], proposed by Lake *et al.* [29], can be used to analyze physiological time series. SampEn quantifies the conditional probability that two sequences of m length similar consecutive data points will still be similar for m+1 (given a tolerance r). DDM generation is an intermediate step for SampEn calculation. DDM consists of similarity degrees which are determined by the distance and a decision rule. The distance is defined as follows:

For the HRV series  $x(i), 1 \leq i \leq N$ , given the parameters m, form  $N - m + 1$  vectors

$$X_i^m = \{x(i), x(i+1), \dots, x(i+m-1)\} \quad 1 \leq i \leq N - m \tag{1}$$

The distance between any two vectors  $X_i^m$  and  $X_j^m$  based on the maximum absolute difference is defined as:

$$d_{i,j}^m = d[X_i^m, X_j^m] = \max_{k=0}^{m-1} |x(i+k) - x(j+k)| \tag{2}$$

where m denotes the embedding dimension.

The decision rule for vector similarity is based on the Heaviside function in SampEn. If the distance is within the threshold parameter r, the similarity degree between the two vectors is 1; if the distance is beyond the threshold parameter r, the similarity degree is 0. This rigid boundary may induce abrupt changes of entropy values when the tolerance threshold r changes slightly, and even fail to define the entropy if no vector-matching could be found [30]–[32]. To enhance the statistical stability, a fuzzy measure entropy (FuzzyMEN) method was proposed [31], [33], which used a fuzzy membership function to substitute the Heaviside function.

Unlike the 0 or 1 discrete determination for vector similarity degree in SampEn, fuzzy membership function permits the FuzzyMEN outputs continuous numerical values between 0 and 1 for the degree of vector similarity. Since FuzzyMEN not only measures the global vector similarity degree, but also refers to the local vector similarity degree. Thus, in

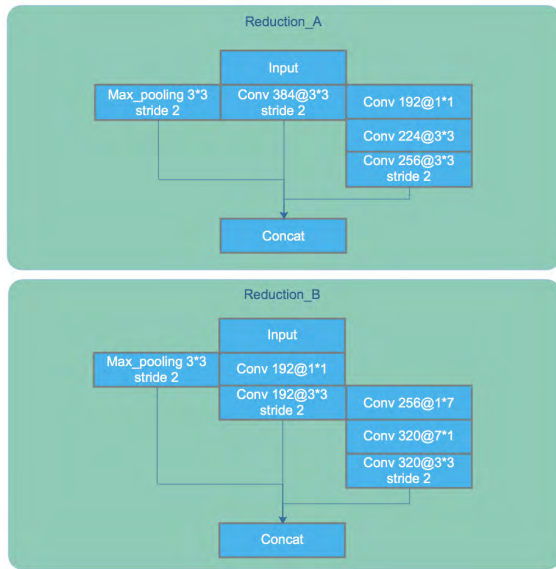


FIGURE 5. "Reduction" module in SE\_Inception\_v4.

this study we define FuzzyLMEn as the FuzzyMEN that is measured by local vector similarity degree. We also use FuzzyGMEn to denote the FuzzyMEN that is measured by global vector similarity degree. The detailed descriptions of SampEn, FuzzyLMEn and FuzzyGMEn were summarized in the Appendix.

Three types of DDMs are generated firstly at the setting of different embedding dimension  $m$  and  $m + 1$ . Then we calculated the difference of these two DDMs. In the following classification process, the differences of DDMs were used as the input images of the CNN classifiers. Figures 6-8 show the DDMs generated by SampEn, FuzzyGMEn and FuzzyLMEn. We set embedding dimension  $m$  as 2 and 3 combined with threshold  $r = 0.1$  and segment length  $N = 300$ , which has been proved statistical significance for SampEn,

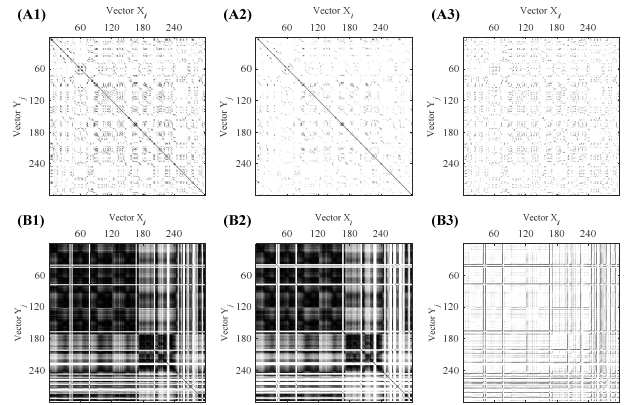


FIGURE 7. (A) DDM generated by FuzzyGMEn for NSR subject under different parameter settings: (A1)  $m = 2$ , (A2)  $m = 3$ , (A3) the difference of (A1) and (A2); (B) DDM generated by FuzzyGMEn for CHF patient under different parameter settings: (B1)  $m = 2$ , (B2)  $m = 3$ , (B3) the difference of (B1) and (B2).

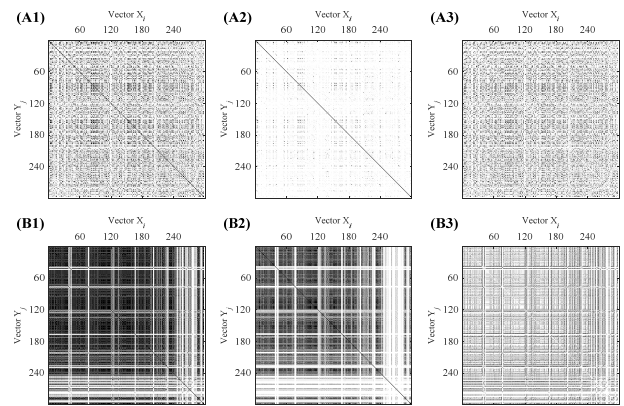


FIGURE 8. (A) DDM generated by FuzzyLMEn for NSR subject under different parameter settings: (A1)  $m = 2$ , (A2)  $m = 3$ , (A3) the difference of (A1) and (A2); (B) DDM generated by FuzzyLMEn for CHF patient under different parameter settings: (B1)  $m = 2$ , (B2)  $m = 3$ , (B3) the difference of (B1) and (B2).

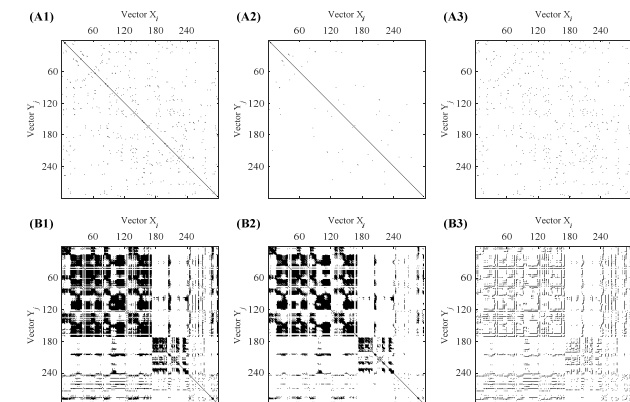


FIGURE 6. (A) DDM generated by SampEn for NSR subject under different parameter settings: (A1)  $m = 2$ , (A2)  $m = 3$ , (A3) the difference of (A1) and (A2); (B) DDM generated by SampEn for CHF patient under different parameter settings: (B1)  $m = 2$ , (B2)  $m = 3$ , (B3) the difference of (B1) and (B2).

FuzzyGMEn and FuzzyLMEn [21]. Only  $1 \leq i \leq 297$  and  $1 \leq j \leq 297$  are shown for illustrating the details. In each sub-figure, the upper panel shows the results from a NSR subject, and the lower panel shows the results from a CHF subject. The results are from the embedding dimension  $m = 2$ , and  $m = 3$  respectively. Their difference is showed from left to right respectively and are used as the input images of the CNN classifiers in the following classification process. Black colored areas indicate the similarity degree = 1 and vice versa.

Figure 6 presents the DDMs generated by SampEn. Figures 7-8 present the DDMs generated by FuzzyGMEn and FuzzyLMEn respectively. Unlike the 0 or 1 discrete determination for vector similarity degree in SampEn, FuzzyGMEn and FuzzyLMEn permit the outputs of continuous real values between 0 and 1 for the vector similarity degree, by converting the absolute distance of using a fuzzy exponential function (see Appendix). Dark-colored areas indicate the higher similarity degree and vice versa.

**D. MODEL CONFIGURATION**

The details of AlexNet, DenseNet and SE\_Inception\_v4 are illustrated in Fig. 1, Fig. 2 and Fig. 3 respectively. All three models were implemented with Tensorflow library [34]. We trained the networks from scratch with a Gaussian random initializer ( $\mu = 0, \sigma = 0.01$ ). The Adam optimizer with an initial learning rate of 0.0001 was used for parameters updating. The dropout was set to 0.5 to avoid overfitting.

**E. EVALUATION SCHEME**

In this study two schemes are considered for the selection of training and test sets. The first selecting scheme is based on subject (recording). We randomly select subjects into five folds. Four folds for training, and the remaining one is for testing. Table 2 shows the results of selecting.

**TABLE 2. Fold results for all records in the two groups.**

Fold#	CHF records	NSR records	Num ber of	Num ber of	Tot al
fold1	201,213,215,218,	8,12,13,20,22,23,25,38	6	11	17
fold2	202,205,206,210,	4,15,21,24,27,29,31,37	6	11	17
fold3	204,207,209,219,	1,7,9,10,11,16,19,34,4	6	11	17
fold4	203,216,217,221,	5,6,17,26,28,32,35,42,	6	11	17
fold5	208,211,212,214,	2,3,14,18,30,33,36,40,	5	10	15
total			29	54	83

Besides subject-based selecting scheme, we also consider segment-based scheme. To evaluate the robustness of the proposed models, 5-fold cross-validation strategy is employed. Firstly, the first 10% data of each subject are used to train and the other 90% of data are used to test without any overlap. Then the percent of train data increases by 10% and repeats until the first 90% data of each subject are used to train and the last 10% are used to test.

**F. PERFORMANCE MEASURES**

We evaluate our model performance by combining True/False Positives/Negatives to measure Precision, Recall and Accuracy (Acc.) [35]. They are often considered to be the most informative for characterizing the performance of a classifier and easy to calculate. Accuracy (Acc.) is the ratio of the total number of positives and negatives correctly made by the recognition system to the actual total number of positives and negatives confirmed by the recognition system. Precision measures the rate of true positives among all detections, while Recall measures the percentage of detected ground truth annotations. They are defined by:

$$\begin{aligned}
 \text{Precision} &= \frac{TP}{TP + FP}, & \text{Recall} &= \frac{TP}{TP + FN}, \\
 \text{Acc.} &= \frac{TP + TN}{TP + TN + FP + FN}
 \end{aligned}
 \tag{3}$$

where true positives (TP) denotes the number of CHF segments correctly classified as CHF group. False positives (FP) refer to the number of NSR segments incorrectly classified as

CHF group. True negatives (TN) associate with the number of NSR segments correctly classified as NSR group. False negatives (FN) refer to the number of CHF segments incorrectly classified as NSR group.

**IV. RESULTS**

**A. SUBJECT-BASED SCHEME**

For the subject-based selecting scheme, Tables 3-5 present the 5-fold cross-validated Precision, Recall, and Mean Acc. under subject-based selecting scheme, resulting from each 3 classifiers (AlexNet, DenseNet, SE\_Inception\_v4) trained by DDMs generated from SampEn, FuzzyGMEn and FuzzyLMEn respectively. The method that reports the best score is SE\_Inception\_v4 trained by FuzzyGMEn-generated DDMs, resulting in Acc. = 81.85% and Std. = 2.97%.

**B. SEGMENT-BASED SCHEME**

Tables 6-8 present the results under segment-based selecting scheme. The method that reports the best score is SE\_Inception\_v4, which trained by global type data,

**TABLE 3. The performance summary using SampEn-generated DDMs based on subject-based scheme.**

DDM generation method	CNN model	Fold #	Precision (%)	Recall (%)	Acc. (%)	Mean Acc. ± Std. (%)
SampEn	AlexNet	fold1	72.95	53.97	76.99	79.81±3.90
		fold2	89.04	71.23	85.32	
		fold3	81.35	41.88	76.90	
		fold4	70.93	50.61	76.08	
		fold5	79.29	59.87	83.75	
SampEn	DenseNet	fold1	67.92	78.35	79.56	78.43±3.04
		fold2	65.14	86.31	76.59	
		fold3	75.48	41.33	75.41	
		fold4	78.45	43.86	76.75	
		fold5	77.42	71.70	83.86	
SampEn	SE_Inception_v4	fold1	76.24	54.25	78.17	80.94±4.10
		fold2	86.67	78.89	87.01	
		fold3	77.09	50.08	77.90	
		fold4	75.23	48.23	76.93	
		fold5	75.69	70.24	84.70	

**TABLE 4. The performance summary using FuzzyGMEn-generated DDMs based on subject-based scheme.**

DDM generation method	CNN model	Fold #	Precision (%)	Recall (%)	Acc. (%)	Mean Acc. ± Std. (%)
FuzzyGMEn	AlexNet	fold1	80.03	49.88	78.20	80.09±2.94
		fold2	86.96	76.06	85.52	
		fold3	85.80	44.95	78.69	
		fold4	76.06	48.76	77.29	
		fold5	78.09	57.41	80.75	
FuzzyGMEn	DenseNet	fold1	81.21	50.54	78.69	77.15±2.02
		fold2	64.99	77.75	74.92	
		fold3	77.51	55.81	79.41	
		fold4	77.91	50.36	78.20	
		fold5	72.87	35.56	74.52	
FuzzyGMEn	SE_Inception_v4	fold1	72.32	67.26	79.62	81.85±2.97
		fold2	86.73	79.02	87.07	
		fold3	77.05	57.72	79.72	
		fold4	81.56	51.77	79.56	
		fold5	86.46	49.74	83.27	

**TABLE 5. The performance summary by FuzzyLMEn-generated DDMs based on subject-based scheme.**

DDM generation method	CNN model	Fold #	Precision (%)	Recall (%)	Acc. (%)	Mean Acc. ± Std. (%)
FuzzyLMEn	AlexNet	fold1	77.13	48.47	77.04	77.83±3.30
		fold2	83.20	73.07	83.70	
		fold3	74.93	42.99	75.65	
		fold4	67.89	52.06	74.11	
		fold5	76.03	50.91	78.63	
FuzzyLMEn	DenseNet	fold1	78.18	52.51	78.35	74.22±3.41
		fold2	81.85	26.80	69.06	
		fold3	72.35	43.94	75.15	
		fold4	76.37	46.62	76.88	
		fold5	75.84	19.86	71.64	
FuzzyLMEn	SE_Inception_v4	fold1	80.50	48.47	77.95	79.46±1.98
		fold2	84.43	69.80	83.16	
		fold3	80.94	45.05	77.64	
		fold4	83.05	47.84	78.88	
		fold5	70.94	64.50	79.69	

**TABLE 6. The performance summary using SampEn-generated DDMs based on segment-based scheme.**

DDM generation method	CNN model	Training Data (%)	Test Data (%)	Precision (%)	Recall (%)	Acc. (%)	Mean Acc. ± Std. (%)
SampEn	AlexNet	10	90	82.35	46.82	77.82	78.05 ±0.85
		20	80	82.27	45.77	77.51	
		30	70	78.42	53.29	78.46	
		40	60	78.17	54.88	78.80	
		50	50	78.10	55.19	78.85	
		60	40	79.59	52.30	78.54	
		70	30	80.51	51.27	78.56	
		80	20	77.67	52.07	77.93	
		90	10	69.35	46.32	75.97	
SampEn	DenseNet	10	90	74.47	48.12	76.01	78.35 ±1.80
		20	80	81.10	41.25	76.01	
		30	70	74.68	63.28	79.59	
		40	60	83.11	45.29	77.58	
		50	50	82.24	41.75	76.40	
		60	40	80.42	55.71	79.68	
		70	30	82.52	56.35	80.51	
		80	20	80.17	60.13	80.78	
		90	10	78.12	53.97	78.55	
SampEn	SE_Inception_v4	10	90	70.08	61.75	77.33	79.28 ±0.97
		20	80	88.49	44.69	78.55	
		30	70	76.21	62.43	79.98	
		40	60	82.05	55.64	80.17	
		50	50	85.20	51.58	79.87	
		60	40	80.83	55.25	79.68	
		70	30	78.02	60.18	80.09	
		80	20	85.03	51.42	79.76	
		90	10	83.22	46.99	78.08	

resulting in Mean Acc. = 80.94% and Std. = 1.71%. Mean accuracies of all 3 trained models score between 78.05% and 80.94%, except for the lowest score of 76.82% generated by SampEn-generated DDMs. It is also shown that the performance for these three models increase greatly when the percent of data to train varies from 10% to 90%.

It is clear that inception-v4 performs the best with the highest mean accuracy for each of the 3 methods and both selecting schemes. It can also be seen that FuzzyGMEn-generated matrixes tend to show a more profound feature

**TABLE 7. The performance summary using FuzzyGMEn-generated DDMs based on segment-based scheme.**

DDM generation method	CNN model	Training Data (%)	Test Data (%)	Precision (%)	Recall (%)	Acc. (%)	Mean Acc. ± Std. (%)
FuzzyGMEn	AlexNet	10	90	84.04	45.67	77.90	79.27±1.04
		20	80	75.33	55.51	78.01	
		30	70	84.00	52.86	79.92	
		40	60	82.87	51.11	79.13	
		50	50	75.40	54.61	77.83	
		60	40	76.02	62.94	80.02	
		70	30	81.96	55.55	80.13	
		80	20	82.42	57.34	80.73	
		90	10	79.97	56.56	79.79	
		FuzzyGMEn	DenseNet	10	90	84.91	
20	80			78.85	42.73	75.88	
30	70			79.04	62.79	81.10	
40	60			80.17	55.14	79.48	
50	50			79.17	54.27	78.95	
60	40			84.27	54.52	80.46	
70	30			79.71	68.74	82.90	
80	20			78.14	68.32	82.16	
90	10			80.99	61.15	81.34	
FuzzyGMEn	SE_Inception_v4			10	90	72.60	54.54
		20	80	78.28	60.29	80.19	
		30	70	80.66	60.65	81.09	
		40	60	82.98	55.87	80.50	
		50	50	86.34	56.01	81.46	
		60	40	75.77	68.88	81.34	
		70	30	82.18	66.74	83.26	
		80	20	85.51	60.81	82.62	
		90	10	79.39	62.68	81.20	

vector for distinguishing CHF and NSR subjects, which are classified with a higher accuracy compared with those of FuzzyLMEn-generated DDMs in Tables 5, 8 and SampEn-generated DDMs in Tables 3, 6, respectively.

**V. DISCUSSION**

In this study, we choose three CNN models for classifying the NSR and CHF patients, and compared their performances. The result shows that no matter what models we choose, the performances of three model have no significant difference. This means the result is not an accidental phenomenon based on one model. We also choose two different schemes to train models. Under the subject-based scheme, training and test data are totally independent. Under segment-based scheme, a certain fraction of each subject’s segments is randomly selected as the training set and the remaining are used as the test set. Previous study has proved models trained by dependent data performed much better than models trained by independent data [28]. However, in this study, the results from the segment-based scheme are similar to the results from the subject-based scheme. This is due to the large intra-subject variability of DDMs.

Over the past years, automatic classifiers have been proposed in diagnosing patients who are suffering CHF. Isler et al. proposed a model based on KNN and wavelet entropy measures of HRV indices [12]. When they used all features to train models, their accuracy is between 78.31% and 84.34%. However, after they used genetic algorithm (GA) for feature selection, they obtained an accuracy as high as 96.39%. However, the method is too complicated for the

**TABLE 8.** The performance summary using FuzzyLMEn-generated DDMs based on segment-based scheme.

DDM generat ion method	CNN model	Train ing Data (%)	Test Data (%)	Precisi on (%)	Recall (%)	Acc. (%)	Mean Acc. ± Std. (%)
FuzzyL MEn	Alex Net	10	90	75.02	39.37	74.13	76.82±1 .30
		20	80	74.87	50.85	76.76	
		30	70	81.30	47.18	77.66	
		40	60	74.73	55.59	77.83	
		50	50	81.97	46.62	77.68	
		60	40	72.88	58.02	77.68	
		70	30	75.19	53.52	77.51	
		80	20	71.01	59.80	77.31	
		90	10	73.08	44.69	74.82	
FuzzyL MEn	Dens eNet	10	90	73.48	46.76	75.40	78.16±1 .56
		20	80	80.34	42.19	76.09	
		30	70	89.68	46.22	79.26	
		40	60	77.72	52.92	78.16	
		50	50	78.68	48.13	77.23	
		60	40	83.25	48.08	78.37	
		70	30	77.10	61.82	80.17	
		80	20	76.15	62.88	80.05	
		90	10	74.64	59.43	78.68	
FuzzyL MEn	SE I ncept ion_v4	10	90	74.06	49.06	76.10	79.73±1 .59
		20	80	72.05	62.85	78.41	
		30	70	74.83	63.89	79.79	
		40	60	81.78	56.43	80.31	
		50	50	82.59	58.73	81.18	
		60	40	75.06	65.50	80.24	
		70	30	80.50	62.40	81.52	
		80	20	74.57	69.48	80.96	
		90	10	79.72	54.16	79.09	

daily monitoring. A classifier based on classification and regression tree (CART) was proposed by Pecchia *et al.* [17] to distinguish CHF patients from NSR subjects. This method is simpler and can be fully understood without advanced mathematical skills. They evaluate the result of CART to choose feature and discriminate CHF patients. It is worth mentioning that they use “tree A” to classify segments and then use “tree B” to classify subjects. Therefore, their final result is to evaluate the performance of classifying subjects.

The difference between our study and other studies is that, we trained the model for CHF segments classification, not for CHF patients classification. In this way, our performance result cannot be compared with their result because we are measuring different things. This research also allowed us a further research direction: seek for the proper ratio of abnormal segments for CHF diagnosis. Jovic and Kuntalp [13] proposed a model based on random forest and combinations of linear and nonlinear features of HRV. They achieved an accuracy of 73% when they only used combinations of entropy calculation result as the input of the classifier. This result can be improved to around 84% by using combinations of linear and non-linear HRV features. This unpromising result by simply using the combinations of entropy calculation can also prove that DDM contains more information than simple entropy calculation. There are also researchers who designed classifiers based on SVM method and combination of several HRV features and reached high accuracy [14]–[16]. Liu *et al.* [15] and Wang *et al.* [14] compared the

contributions of different combinations of HRV features to performance of classifiers. Liu *et al.* reached a highest accuracy of 91.49% using combination of time domain and non-linear features, which is consistent with the conclusion of Jovic and Bogunovic [13].

All these studies are using multiple features as the input of classifiers, for the reason that the performance with single feature is far poorer. Jovic and Bogunovic [13] achieved results between 60% and 75% which are far lower than other results by using combination of the same type of features, such as approximate entropy (ApEn1–ApEn4), maximum approximate entropy (MaxApEn), multiscale sample entropy (SampEn1–SampEn20), multiscale carnap 1D entropy(Carnap1–Carnap20). The above features all belong to the entropy method category but their calculation methods are different. The result of previous studies depends on which feature set is chosen. However, this best choice may change when choosing different datasets. Additionally, it is also too complex and demanding for the daily activity of clinicians.

## VI. CONCLUSION

In our study, we only used one feature to train models and obtained the highest accuracy of 81.85%. This result is much higher compared to the result of using combination of the same type of features. However, it is much lower than the previous studies which are using combinations of different features. For the next step, we plan to add other dimension images to improve the completeness of input and we expect the result will be improved. Single dimension of input is still too ‘thin or lean’ for a model to train, which can be seen in the current result. Adding more dimension images does not mean we will increase steps of feature selection, since it is CNN itself that extract features. We can also train the CNN classifier using larger dataset, for the reason that small datasets will cause the deep neural network to overfit.

## APPENDIX

### A. SAMPLE ENTROPY METHOD (SAMPEN)

For RR segment  $x(i)$  ( $1 \leq i \leq N$ ), form the vector sequences  $X_i^m$ :

$$X_i^m = \{x(i), x(i+1), \dots, x(i+m-1)\},$$

$$1 \leq i \leq N - m + 1$$

Then the distance between  $X_i^m$  and  $X_j^m$  based on the maximum absolute difference is defined as:

$$d_{i,j}^m = d[X_i^m, X_j^m] = \max_{k=0}^{m-1} |x(i+k) - x(j+k)|$$

In SampEn, if the distance is within the threshold parameter  $r = 0.2$ , the similarity degree between the two vectors is 1; if the distance is beyond the threshold parameter  $r$ , the similarity degree is 0. There is absolutely a 0 or 1 determination.

### B. FUZZY MEASURE ENTROPY (FUZZYMEN)

For RR segment  $x(i)$  ( $1 \leq i \leq N$ ), firstly form the local vector sequences  $XL_i^m$  and global vector sequences  $XG_i^m$



respectively:

$$\begin{aligned} XL_i^m &= \{x(i), x(i+1), \dots, x(i+m-1)\} - \bar{x}(i) \\ XG_i^m &= \{x(i), x(i+1), \dots, x(i+m-1)\} - \bar{x} \\ 1 &\leq i \leq N - m \end{aligned}$$

The vector  $XL_i^m$  represents  $m$  consecutive  $x(i)$  values but removing the local baseline  $\bar{x}(i)$ , which is defined as:

$$\bar{x}(i) = \frac{1}{m} \sum_{k=0}^{m-1} x(i+k) \quad 1 \leq i \leq N - m$$

The vector  $XG_i^m$  also represents  $m$  consecutive  $x(i)$  values but removing the global mean value  $\bar{x}$  of the segment  $x(i)$ , which is defined as:

$$\bar{x} = \frac{1}{N} \sum_{i=1}^N x(i)$$

Then the distance between the local vector sequences  $XL_i^m$  and  $XL_j^m$  and the distance between the global vector sequences  $XG_i^m$  and  $XG_j^m$  are defined as follows respectively:

$$\begin{aligned} dL_{i,j}^m &= d[XL_i^m, XL_j^m] \\ &= \max_{k=0}^{m-1} |(x(i+k) - \bar{x}(i)) - (x(j+k) - \bar{x}(j))| \\ dG_{i,j}^m &= d[XG_i^m, XG_j^m] \\ &= \max_{k=0}^{m-1} |(x(i+k) - \bar{x}) - (x(j+k) - \bar{x})| \end{aligned}$$

Given the parameters  $n_L$ ,  $r_L$ ,  $n_G$  and  $r_G$ , calculate the similarity degree  $DL_{i,j}^m(n_L, r_L)$  between the local vectors  $XL_i^m$  and  $XL_j^m$  by the fuzzy function  $\mu L(dL_{i,j}^m, n_L, r_L)$ , as well as calculate the similarity degree  $DG_{i,j}^m(n_G, r_G)$  between the global vectors  $XG_i^m$  and  $XG_j^m$  by the fuzzy function  $\mu G(dG_{i,j}^m, n_G, r_G)$ :

$$\begin{aligned} DL_{i,j}^m(n_L, r_L) &= \mu L(dL_{i,j}^m, n_L, r_L) = \exp\left(-\frac{(dL_{i,j}^m)^{n_L}}{r_L}\right) \\ DG_{i,j}^m(n_G, r_G) &= \mu G(dG_{i,j}^m, n_G, r_G) = \exp\left(-\frac{(dG_{i,j}^m)^{n_G}}{r_G}\right) \end{aligned}$$

In this study, the local similarity weight  $n_L = 1$  and global vector similarity weight  $n_G = 2$ , the local tolerance threshold  $r_L$  was set equal to the global threshold  $r_G$ , i.e.,  $r_L = r_G = r$ .

## ACKNOWLEDGMENT

(Yaowei Li, Yao Zhang, Lina Zhao, and Yang Zhang are co-first authors.)

## REFERENCES

- J. K. Ghali, R. Cooper, and E. Ford, "Trends in hospitalization rates for heart failure in the United States, 1973-1986. Evidence for increasing population prevalence," *Arch. Internal Med.*, vol. 150, no. 4, pp. 769-773, 1990.
- R. F. Gillum, "Heart failure in the United States 1970-1985," *Amer. Heart J.*, vol. 113, no. 4, pp. 1043-1045, 1987.
- A. Mosterd and A. W. Hoes, "Clinical epidemiology of heart failure," *Heart*, vol. 93, no. 9, pp. 1137-1146, 2007.
- D. D. Schocken, M. I. Arrieta, P. E. Leaverton, and E. A. Ross, "Prevalence and mortality rate of congestive heart failure in the United States," *J. Amer. College Cardiol.*, vol. 20, no. 2, pp. 301-306, 1992.
- F. Hobbs, J. Doust, J. Mant, and M. R. Cowie, "Diagnosis of heart failure in primary care," *Heart*, vol. 96, no. 21, pp. 1773-1777, 2010.
- R. Cardarelli and T. G. Lumicao, Jr., "B-type natriuretic peptide: A review of its diagnostic, prognostic, and therapeutic monitoring value in heart failure for primary care physicians," *J. Amer. Board Family Pract.*, vol. 16, no. 4, pp. 327-333, 2003.
- A. Fuat, A. P. S. Hungin, and J. J. Murphy, "Barriers to accurate diagnosis and effective management of heart failure in primary care: Qualitative study," *Brit. Med. J.*, vol. 326, no. 7382, p. 196, 2003.
- J. Remes, H. Miettinen, A. Reunanen, and K. Pyörälä, "Validity of clinical diagnosis of heart failure in primary health care," *Eur. Heart J.*, vol. 12, no. 3, pp. 315-321, 1991.
- J. Nolan et al., "Prospective study of heart rate variability and mortality in chronic heart failure: Results of the United Kingdom heart failure evaluation and assessment of risk trial (UK-heart)," *Circulation J.*, vol. 98, no. 15, pp. 1510-1516, 1998.
- M. Hadase et al., "Very low frequency power of heart rate variability is a powerful predictor of clinical prognosis in patients with congestive heart failure," *Circulation J.*, vol. 68, no. 4, pp. 343-347, 2004.
- M. T. La Rovere et al., "Short-term heart rate variability strongly predicts sudden cardiac death in chronic heart failure patients," *Circulation*, vol. 107, no. 4, pp. 565-570, Feb. 2003.
- Y. İşler and M. Kuntalp, "Combining classical HRV indices with wavelet entropy measures improves to performance in diagnosing congestive heart failure," *Comput. Biol. Med.*, vol. 37, no. 10, pp. 1502-1510, 2007.
- A. Jovic and N. Bogunovic, "Random forest-based classification of heart rate variability signals by using combinations of linear and nonlinear features," in *Proc. 12th Medit. Conf. Med. Biol. Eng. Comput. Chalkidiki, Greece: Springer*, 2010, pp. 29-32.
- Y. Wang et al., "Comparison of time-domain, frequency-domain and non-linear analysis for distinguishing congestive heart failure patients from normal sinus rhythm subjects," *Biomed. Signal Process. Control*, vol. 42, pp. 30-36, Apr. 2018.
- L. Liu, L. Wang, Q. Wang, G. Zhou, Y. Wang, and Q. Jiang, "A new approach to detect congestive heart failure using short-term heart rate variability measures," *PLoS ONE*, vol. 9, no. 4, p. e93399, 2014.
- G. Yang et al., "A heart failure diagnosis model based on support vector machine," in *Proc. 3rd Int. Conf. Biomed. Eng. Inform. (BMEI)*, vol. 3, Oct. 2010, pp. 1105-1108.
- L. Pecchia, P. Melillo, M. Sansone, and M. Bracale, "Discrimination power of short-term heart rate variability measures for CHF assessment," *IEEE Trans. Inf. Technol. Biomed.*, vol. 15, no. 1, pp. 40-46, Jan. 2011.
- S. M. Pincus and A. L. Goldberger, "Physiological time-series analysis: What does regularity quantify?" *Amer. J. Physiol.-Heart Circulatory Physiol.*, vol. 266, no. 4, pp. H1643-H1656, 1994.
- J. S. Richman and J. R. Moorman, "Physiological time-series analysis using approximate entropy and sample entropy," *Amer. J. Physiol.-Heart Circulatory Physiol.*, vol. 278, no. 6, pp. H2039-H2049, 2000.
- R. Barbieri, E. P. Scilingo, and G. Valenza, *Complexity and Nonlinearity in Cardiovascular Signals*. Cham, Switzerland: Springer, 2017.
- L. Zhao et al., "Determination of sample entropy and fuzzy measure entropy parameters for distinguishing congestive heart failure from normal sinus rhythm subjects," *Entropy*, vol. 17, no. 12, pp. 6270-6288, 2015.
- C. Liu and R. Gao, "Multiscale entropy analysis of the differential RR interval time series signal and its application in detecting congestive heart failure," *Entropy*, vol. 19, no. 6, p. 251, 2017.
- A. L. Goldberger et al., "PhysioBank, PhysioToolkit, and PhysioNet: Components of a new research resource for complex physiologic signals," *Circulation*, vol. 101, no. 23, pp. 215-220, 2000.
- A. Krizhevsky, I. Sutskever, and G. E. Hinton, "Imagenet classification with deep convolutional neural networks," in *Proc. Adv. Neural Inf. Process. Syst.*, 2012, pp. 1097-1105.
- G. Huang, Z. Liu, K. Q. Weinberger, and L. van der Maaten, "Densely connected convolutional networks," in *Proc. IEEE Conf. Comput. Vis. Pattern Recognit.*, vol. 1, Jun. 2017, pp. 4700-4708.
- C. Szegedy, S. Ioffe, V. Vanhoucke, and A. A. Alemi, "Inception-v4, inception-resnet and the impact of residual connections on learning," in *Proc. Artif. Intell. (AAAI)*, 2017, pp. 4278-4284.
- C. Szegedy et al., "Going deeper with convolutions," in *Proc. Eur. Conf. Comput. Vis.*, Jun. 2015, pp. 1-9.

- [28] Q. Qin, J. Li, L. Zhang, Y. Yue, and C. Liu, "Combining low-dimensional wavelet features and support vector machine for arrhythmia beat classification," *Sci. Rep.*, vol. 7, Jul. 2017, Art. no. 6067.
- [29] D. E. Lake, J. S. Richman, M. P. Griffin, and J. R. Moorman, "Sample entropy analysis of neonatal heart rate variability," *Amer. J. Physiol.-Regulatory Integrative Comparative Physiol.*, vol. 283, no. 3, pp. R789–R797, 2002.
- [30] W. T. Chen, J. Zhuang, W. X. Yu, and Z. Z. Wang, "Measuring complexity using FuzzyEn, ApEn, and SampEn," *Med. Eng. Phys.*, vol. 31, no. 1, pp. 61–68, 2009.
- [31] C. Y. Liu et al., "Analysis of heart rate variability using fuzzy measure entropy," *Comput. Biol. Med.*, vol. 43, no. 2, pp. 100–108, 2013.
- [32] M. U. Ahmed and D. P. Mandic, "Multivariate multiscale entropy: A tool for complexity analysis of multichannel data," *Phys. Rev. E, Stat. Phys. Plasmas Fluids Relat. Interdiscip. Top.*, vol. 84, no. 6, p. 061918, 2011.
- [33] C. Y. Liu and L. N. Zhao, "Using fuzzy measure entropy to improve the stability of traditional entropy measures," in *Proc. Comput. Cardiol.*, Hangzhou, China, Sep. 2011, pp. 681–684.
- [34] M. Abadi et al. (2015). *TensorFlow: Large-Scale Machine Learning on Heterogeneous Distributed Systems*. [Online]. Available: [www.tensorflow.org](http://www.tensorflow.org)
- [35] D. M. W. Powers, "Evaluation: From precision, recall and F-measure to ROC, informedness, markedness & correlation," *J. Mach. Learn. Technol.*, vol. 2, no. 1, pp. 37–63, 2011.



**YAOWEI LI** received the B.S. degree in mathematics and applied mathematics from Shandong Normal University, China, in 2017. She is currently a Research Assistant with the Southeast-Lenovo Wearable Heart-Sleep-Emotion Intelligent Monitoring Lab, Southeast University, China. Her research interests include artificial intelligence, machine learning, and deep learning.



**YAO ZHANG** received the B.S. degree from Harbin Engineering University, Harbin, China, in 2015. He is currently pursuing the Ph.D. degree with the Institute of Computing Technology, Chinese Academy of Sciences. His research interests include medical image analysis, deep learning, and computer-aided diagnosis.



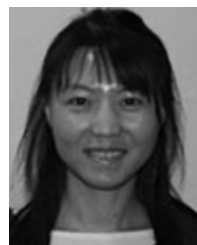
**LINA ZHAO** received the B.S. and M.S. degrees in biomedical engineering from Shandong University, Jinan, China, in 2005 and 2008, respectively, where she is currently pursuing the Ph.D. degree with the School of Control Science and Engineering. She was a Researcher with the Shandong Heng-Xin Inspection Technique Exploiture Center, Jinan. Her research interests include entropy methods for physiological signal analysis, ECG, PCG, and artery pressure pulse processing.



**YANG ZHANG** received the master's and Ph.D. degrees from Northumbria University, Newcastle upon Tyne, U.K. He is currently an Advisory Researcher with Lenovo Research, Beijing. He holds expertise and experience in computer vision, medical imaging, affective computing, and natural language processing. His major interests remain in the fields of artificial intelligence, pattern recognition, and deep learning.



**CHENGYU LIU** (M'13) received the B.S. and Ph.D. degrees in biomedical engineering from Shandong University, China, in 2005 and 2010, respectively. He has completed the post-doctoral trainings at Shandong University, China, from 2010 to 2013, Newcastle University, U.K., from 2013 to 2014, and Emory University, USA, from 2015 to 2017. He is currently a Professor with the School of Instrument Science and Engineering, Southeast University, China. He is also the Director of the Southeast-Lenovo Wearable Heart-Sleep-Emotion Intelligent Monitoring Lab. He was the PI on over 10 awarded grants. He has published over 130 papers. His research topics include mHealth and intelligent monitoring, machine learning and big data processing for cardiovascular signals, device development for CADs, and sleep and emotion monitoring. He is a Federation Journal Committee Member of the International Federation for Medical and Biological Engineering. He is also the Chair of the China Physiological Signal Challenge 2018.



**LI ZHANG** (M'11) received the Ph.D. degree from the University of Birmingham, U.K. She is currently an Associate Professor and a Reader in computer science with Northumbria University, U.K. She holds expertise in artificial intelligence, machine learning, intelligent robotics, and deep learning. She is also serving as an Honorary Research Fellow with the University of Birmingham. She has served as an Associate Editor for *Decision Support Systems*.



**LIUXIN ZHANG** received the B.S. and Ph.D. degrees in computer science and technology from the Beijing Institute of Technology, China, in 2004 and 2010, respectively. He joined Lenovo Research in 2010, where he is currently serving as a Senior Researcher and the Senior Manager with the responsibility of leading Lenovo User Experience Research Team and Human-Computer Interaction Team. His research interests were focused on computer vision and human-computer interaction. He is also the Committee Member of the Human-Computer Interaction Branch, China Computer Federation.



**ZHENSHEG LI** received the B.S. and M.S. degrees in management information system from the Renmin University of China, in 2005 and 2010, respectively. He successfully drove Lenovo Research to build up the Southeast University-Lenovo Wearable Heart-Sleep-Emotion Intelligent Monitoring Lab, and joined the National Engineering Laboratory of Medical Big Data Application Technology. He is currently the Project Research Manager with Lenovo Research. His research fields include big data, computer vision, and mHealth.



**BINHUA WANG** received the M.S. and Ph.D. degrees in biomedical engineering from Shandong University, China, in 2011 and 2016, respectively. He was as an Assistant with the Translational Medical Center, Chinese PLA General Hospital, Beijing, China, where he holds a post-doctoral position at the Medical Big Data Center. His research interests include heart failure database construction and application research, artificial intelligence research based on medical imaging, and sleep data analysis and application.



**EYK NG** received the Ph.D. degree from Cambridge University with a Cambridge Commonwealth Scholarship. He is currently a Faculty Member with the College of Engineering, Nanyang Technological University, Singapore. His main areas of research are thermal imaging, human physiology, biomedical engineering, computational fluid dynamics, and numerical heat transfer. He has been the lead Editor-in-Chief of the *Journal of Mechanics in Medicine and Biology* since 2000. He is the Founding Editor-in-Chief of the *Journal of Medical Imaging and Health Informatics* and an associate editor of EAB of various referred international journals, such as *Artificial Intelligence*, *BioMedical Engineering OnLine*, and the *Journal of Advanced Thermal Science Research*.



**JIANQING LI** received the B.S. and M.S. degrees in automatic technology from the School of Instrument Science and Engineering, Southeast University, China, in 1986 and 1992, respectively, and the Ph.D. degree in measurement technology and instruments from Southeast University. He is currently a Professor with the School of Basic Medical Sciences, Nanjing Medical University, China, where he is also the Vice President. He is currently a Professor with the School of Instrument Science and Engineering, Southeast University. His research topics include mHealth, wearable ECG systems, multi-parameter physiological signal detection, and wireless networks.



**ZHIQIANG HE** is currently the Senior Vice President of Lenovo Research and the President of the Lenovo Capital and Incubator Group. This group is responsible for exploring external innovation, accelerating internal innovation for Lenovo Group, and leveraging Lenovo global resources, power of capital, and entrepreneurship. Previously, he was the Chief Technology Officer and held various leadership positions in Lenovo Research, particularly in overseeing Lenovo's Research and Technology initiatives and systems. He is also a Doctoral Supervisor with the Institute of Computing Technology, Chinese Academy of Sciences, and Beihang University.

...